Aerospace Science and Technology 55 (2016) 64–75

Contents lists available at ScienceDirect

Aerospace Science and Technology

www.elsevier.com/locate/aescte

Pseudo-analytic approach to determine optimal conditions for maximizing altitude of sounding rocket

Sang-Hyeon Lee

Dept. of Mechanical Eng., University of Ulsan, Ulsan, 680-749, Republic of Korea

ARTICLE INFO

Article history:
Received 24 February 2016
Received in revised form 10 May 2016
Accepted 17 May 2016
Available online 19 May 2016

ABSTRACT

A pseudo-analytic approach is suggested to determine the optimal launching conditions for maximizing the altitude of a sounding rocket flying with a constant mass flow of propellant in a standard atmosphere. The one-dimensional rocket momentum equation including thrust, gravitational force, and aerodynamic drag is considered, for which it is impossible to obtain the analytic solutions since the governing equation is nonlinear. The piecewise pseudo-analytic solutions are obtained with a constant control parameter introduced to make the velocity integral in the governing equation be analytic. The rocket flight in the standard atmosphere is analyzed by dividing the entire range into small intervals where the drag parameter or the gravitational acceleration can be treated as a constant in each interval. The pseudo-analytic approach gives precise predictions of the rocket velocity and the rocket altitude that agree well with the numerical ones. A characteristic equation exists and provides accurate predictions of the optimal mass flow rate for maximizing the altitude at burn-out state or at apogee.

1. Introduction

Many countries use sounding rocket programs in an effort to develop technologies related to sounding rockets, since scientific studies employing such programs are simple, efficient, and inexpensive compared to those with a satellite [1–12]. Most scientific measurements, observations, or experiments for sounding rocket missions are carried out near apogee. This is the case because the low speed near apogee provides unique opportunities to explore or observe the surrounding space in a short time period. Furthermore, there are some important regions of space that are too close to the earth's surface to be sampled by satellites; however, sounding rockets provide platforms for carrying out in-situ measurements in these regions [9]. Some microgravity environments [13,14] are carried after burn-out state and some scramjet experiments [15,16] are conducted during free-fall which provides a good hypersonic condition at a low cost. Therefore, the design target of a sounding rocket is the altitude at burn-out state or apogee. The rocket altitude can change based on the ejection conditions of the propellant jet. Therefore, it is necessary to determine an optimal condition for maximizing the altitude for given launching conditions.

The Goddard problem of optimal thrust programming for maximizing the altitude of a rocket in vertical flight has been extensively studied using variation methods, asymptotic approaches or optimal control theories [17–20]. These are not based on the analytic solution of the rocket momentum equation, since there is no general analytic solution due to the nonlinearity of the governing equation. There are also approximate solutions using the Taylor series expansion, the perturbation method or the least square method [21], but they are complex and do not provide information about the optimal conditions. An analytic exact solution of the rocket momentum equation including thrust, gravitational force and aerodynamic drag force exists only in a typical situation where the three forces are well balanced. A previous study [22] presented an analytic approach to obtain analytic solution and to determine the optimal conditions for the typical situations. This approach was extended to rocket flight in a standard atmosphere [23]. However the existence of an analytic solution requires the balance of the three forces and thus the typical control of the mass flow rate of propellant. Thus these analytic approaches have serious limitations in real applications. For instance, most sounding rockets use a constant mass flow rate of propellant in which the rocket motion cannot be solved with an analytic approach. Hence, in the present study, a pseudo-analytic approach to obtain an approximate solution and determine the optimal conditions for maximizing the altitude of a sounding rocket are suggested and verified.

We consider the motion of a sounding rocket launched in the vertical direction for simplicity. Then, the motion of a sounding rocket can be described using a one-dimensional momentum equation that includes thrust, gravitational force, and aerodynamic drag force. The rocket mass varies with time, and the aerodynamic drag

E-mail address: lsh@mail.ulsan.ac.kr.

http://dx.doi.org/10.1016/j.ast.2016.05.013
1270-9638/

Nomenclature

F	= thrust
G	= ratio between inertia and drag
g	= gravitational acceleration
h	= altitude
J	= pseudo drag parameter
K	= drag parameter
M	= Mach number
m	= rocket mass
$\dot{m}$	= rate of rocket mass change or mass flow rate of propellant jet
q	= velocity parameter for rocket velocity
r	= control parameter for rocket velocity
t	= time
u	= velocity of propellant jet
v	= rocket vertical velocity
p	= static pressure
T	= temperature
γ	= specific heats ratio
ρ	= density
Ω	= rocket mass ratio between total mass and dry-mass
ω	= rocket mass ratio between adjacent intervals

Subscripts

a	= ambient air
b	= burn-out state
c	= rocket combustor
e	= jet condition at rocket nozzle exit
o	= ground state
opt	= optimal condition for maximizing altitude
s	= stationary state (apogee)

is proportional to the square of the rocket velocity, which makes the governing equation nonlinear. Thus, we cannot obtain an analytic solution in a general form. We also consider the case where the mass flow rate of propellant is constant for which analytic solutions of the rocket momentum equation do not exist. We cannot use the analytic approaches, but there is a possibility to extend the previous analytic approaches [22,23] to build a pseudo-analytic approach for finding solutions. The reason why we cannot obtain analytic solutions is that the governing differential equation cannot be integrated in an analytic way. However, if the governing equation is multiplied by a proper parameter, one side of the differential equation can be analytically integrated. On the other hand, the other side of the governing differential equation cannot be integrated in an analytic way. A similar situation occurs when we deal with rocket flight in the standard atmosphere [24], where the air density dramatically changes with the altitude. Further, the gravitational acceleration cannot be treated as a constant when rockets reach the upper atmosphere. Moreover, the aerodynamic drag coefficient changes with the flight Mach number especially around the Mach number of unity. Hence, the aerodynamic drag is a variable that changes with the altitude or rocket velocity. A previous study [23] shows that the "divide-and-conquer" strategy might be a way to avoid these serious issues. Hence, we can exploit this strategy to solve the problem in the present study. If we divide the entire flight range into intervals that are small enough, we can treat the following terms as constants in each interval: the parameter multiplied to both sides of the governing equation, the air density, the gravitational acceleration and the drag coefficient. We can then have piecewise pseudo-analytic solutions and also determine the optimal conditions at burn-out state or apogee.

The rocket model considered in the present study is the same one in the previous study [23] that is a simplified model based on the Korea Sounding Rocket Program (KSR II and III) [8]. KSR II is a solid propellant rocket with a total the weight of 2.0 ton, a diameter of 0.42 m and a length of 11.0 m. KSR III is a liquid propellant rocket with a weight of 6.1 ton, a diameter of 1.0 m and a length of 13.5 m. In the present study, we consider the medium specification between KSR II and KSR III.

In Section 2, the one-dimensional rocket equation in boost phase and coast phase are briefly described. Section 3.1 provides alternative approach to obtain a pseudo-analytic solution of the governing equation. Sections 3.2 and 3.3 show how to build the characteristic equations to obtain the optimal conditions for maximizing altitude at burn-out state and at apogee. Section 4 shows the procedure of the numerical discretization of the governing equation. Section 5 provides calculation conditions such as atmosphere, aerodynamic drag coefficient and launching conditions. Results of calculations are discussed in Section 6.

2. One-dimensional rocket equation

2.1. Governing equation in boost phase

The motion of a rocket in boost phase climbing in the vertical direction can be described with the following one-dimensional rocket equation including thrust and aerodynamic drag as follows [25,26]:

$$m\frac{dv}{dt} = F - mg - Kv^2, \tag{2.1a}$$

$$F = \dot{m}u_e + A_e(p_e - p_a), \tag{2.1b}$$

$$K = \frac{S}{2}C_d\rho_a. \tag{2.1c}$$

The mass flow rate $\dot{m}$ is equal to the rate of the rocket mass change and has a negative sign. In the present study, we consider the cases with a constant mass flow rate of propellant.

$$\dot{m} = \frac{dm}{dt} = const. \tag{2.2a}$$

The mass of a rocket decreases with the mass flow of propellant.

$$m = m_o + \int_o^t \dot{m}dt = m_o + \dot{m}t. \tag{2.2b}$$

If we use the constant specific heats ratio, the mass flow rate through a supersonic nozzle is determined as follows:

$$\dot{m} = \sqrt{\frac{\gamma}{R}\left(\frac{2}{\gamma+1}\right)^{\frac{\gamma+1}{\gamma-1}}}A_{th}\frac{p_c}{\sqrt{T_c}}. \tag{2.2c}$$

The subscript th denotes the throat of a rocket nozzle.

The term A_e in equation (2.1b) is the cross-sectional area at the nozzle exit. For an adiabatic nozzle flow, the total enthalpy is constant, and we can then assume that the jet velocity u_e and the pressure at exit are constant. However, the ambient pressure decreases with the altitude and thus the second term of the thrust increases with the altitude. The jet velocity has a negative sign since its direction is opposite of the rocket velocity; thus, the thrust term $\dot{m}u_e$ has a positive sign.

If the Mach number at the nozzle exit is given, the temperature, pressure, jet velocity and nozzle area at the nozzle exit are determined as follows:

$$T_e = T_c\left(1+\frac{\gamma-1}{2}M_e^2\right)^{-1}, \tag{2.3a}$$

$$p_e = p_c\left(1+\frac{\gamma-1}{2}M_e^2\right)^{\frac{-\gamma}{\gamma-1}}, \tag{2.3b}$$

$$u_e = M_e\sqrt{\gamma R T_e}, \tag{2.3c}$$

$$A_e = \frac{A_{th}}{M_e}\left(\frac{2}{\gamma+1}+\frac{\gamma-1}{\gamma+1}M_e^2\right)^{\frac{\gamma+1}{2(\gamma-1)}}. \tag{2.3d}$$

The terms S and C_d in equation (2.1c) are the cross-sectional area of a rocket body and the aerodynamic drag coefficient, respectively. The air density in a standard atmosphere is not a constant but changes with the altitude. The aerodynamic drag coefficient increases sharply near the Mach number of unity and after then decreases gradually with increasing Mach number [21,27,28]. Hence, the drag parameter K changes with the altitude and the flight Mach number.

$$K = K(h, M). \tag{2.4}$$

We adopt a modified model for estimating the aerodynamic drag coefficient that guarantees smooth changes of the coefficient at all Mach numbers. The details will be presented in section 5.3.

The change in the gravitational force based on the altitude should be considered for high altitude sounding rockets. In the present study, the following relation is used.

$$g = g_o\frac{R_E^2}{(R_E+h)^2}. \tag{2.5}$$

The terms g_o and R_E in equation (2.5) are the gravitational acceleration and average radius of the earth at sea level, which are 9.8067 m/s^2 and 6.371×10^6 m, respectively.

As shown in previous studies [22,23], by introducing a velocity parameter, the governing equation can be expressed as follows:

$$\frac{dv}{q^2-v^2} = \frac{K}{\dot m}\frac{dm}{m}, \tag{2.6a}$$

$$q = \sqrt{\frac{F-mg}{K}} = \sqrt{\frac{\dot m u_e + A_e(p_e-p_a)-mg}{K}}. \tag{2.6b}$$

In the previous studies [22,23], the thrust based on the pressure difference was ignored since the term has only minor effects on the total thrust and it also raises some difficulties in manipulating the formulation. In the present study, the pressure thrust is taken into account for real situations.

If the mass flow rate is constant, the left hand side of equation (2.6a) cannot be analytically integrated since the velocity parameter changes with the mass, the drag parameter or the ambient pressure as shown in equation (2.6b). Thus, we cannot obtain analytic solutions for the governing equation and subsequently we would like to find a way to obtain pseudo-analytic solutions by replacing the velocity parameter with a constant control parameter. This will be discussed in section 3.1.

Even though we could find a way to integrate the left hand side of the governing equation (2.6a) in a pseudo-analytic way, the right hand side of the governing equation cannot be analytically integrated over the entire flight time since the drag parameter changes with the altitude or the Mach number. Thus the right hand side of the governing equation could not be expressed as an explicit function of the time or the mass. Hence, we could not obtain analytic solutions valid for the entire flight time. As a result, we have to find another way to avoid such serious difficulties, such as extending the "divide-and-conquer" strategy. This will be discussed in section 3.1.

2.2. Governing equation in coast phase

After the propellant of a rocket is totally consumed, the flight phase turns into coast phase, where the rocket climbs with inert force until the stationary state or apogee. The rocket equation then becomes

$$m_b\frac{dv}{dt} = -Kv^2 - m_b g. \tag{2.7a}$$

Separating variables leads to

$$\frac{vdv}{Kv^2+m_b g} = -\frac{1}{m_b}dh. \tag{2.7b}$$

An analytic solution of the above equation can be obtained if and only if the drag parameter is constant. As mentioned in the above section, we could not obtain analytic solutions valid for the entire flight time since the drag parameter cannot be expressed as an explicit function of the velocity. This will be discussed in detail in the next section.

3. Pseudo-analytic approaches

3.1. Solution of the governing equation

3.1.1. Solution in boost phase

The velocity parameter q can be replaced with a constant control parameter r to allow the left hand side of the following governing equation to be analytically integrated. The governing equation can then be represented as follows:

$$\frac{dv}{r^2-v^2} = \frac{J}{\dot m}\frac{dm}{m}, \tag{3.1.1a}$$

$$J = K\frac{q^2-v^2}{r^2-v^2}. \tag{3.1.1b}$$

The control parameter r should have a velocity dimension to maintain a consistency of the governing equation. The control parameter should be determined not to make any singularity in the governing equation and thus be greater than the rocket velocity at burn-out state, since a rocket has the maximum velocity at burn-out state. Considering that the goal of the present study is to determine the optimal mass flow rate of propellant, the following definition is a reasonable candidate.

$$r = \sqrt{\frac{\dot m u_e}{K_*}}. \tag{3.1.2a}$$

The critical drag parameter K_* can be an arbitrary constant. However, if the critical drag parameter is determined to satisfy the relation that $J_b = K_b$, we can guarantee a smooth phase transition of the governing equations from boost phase to coast phase and provide a control parameter greater than the rocket velocity at burn-out state. Thus we take the following definition of the critical drag coefficient from equations (2.6b) and (3.1.1b).

$$K_* = K_b\left(1+\frac{A_e(p_e-p_{a,b})-m_b g_b}{\dot m u_e}\right)^{-1}. \tag{3.1.2b}$$

The velocity parameter q then can be expressed as functions of the control parameter as follows:

$$q = r\sqrt{\frac{K_*}{K}\left[1+\frac{A_e(p_e-p_a)-mg}{\dot{m}u_e}\right]}$$
$$= r\sqrt{\frac{K_*}{K}\left[1+\frac{A_e(p_e-p_a)-mg}{K_* r^2}\right]}. \quad (3.1.2c)$$

The parameter J in equation (3.1.1b) changes with the rocket velocity or the velocity parameter. Hence we cannot obtain analytic integration of the right hand side even though the drag coefficient is constant. At this point, we can exploit the strategy of divide-and-conquer [23] to obtain piecewise pseudo-analytic solutions in a similar way. If we divide the entire range into small intervals where the parameter J can be treated as a constant in each interval, we can obtain a pseudo-analytic integration of the right hand side of the above equation.

Then, the governing equation integrated from ground state to the (n) state can be represented as follows:

$$\int_o^n \frac{dv}{r^2-v^2} = \sum_{i=1}^{n} \frac{\bar{J}_i}{\dot{m}} \int_{i-1}^{i} \frac{dm}{m}. \quad (3.1.3a)$$

The over-bar placed over the parameter J denotes the mean value of the parameter in the interval between the $(n-1)$ and (n) states as follows:

$$\bar{J}_n = \frac{J_{n-1}+J_n}{2}. \quad (3.1.3b)$$

The term with an over-bar will be treated as a constant in the interval.

The rocket mass ratio and piecewise mass ratio between masses at the $(n-1)$ and (n) states are defined as follows:

$$\Omega = \frac{m_o}{m_b} > 1, \quad (3.1.4a)$$
$$\omega_n = \frac{m_{n-1}}{m_n} > 1. \quad (3.1.4b)$$

Hence integrating the governing equation (3.1.1) from ground state to the (n) state with the strategy of divide-and-conquer yields

$$\frac{1}{2r}\ln\left(\frac{r+v_n}{r-v_n}\right) = -\frac{1}{\dot{m}}\sum_{i=1}^{n}\bar{J}_i \ln(\omega_i). \quad (3.1.5)$$

Rearranging this equation leads to

$$v_n = r\frac{x_n-1}{x_n+1}, \quad (3.1.6a)$$
$$x_n = \exp\left[-\frac{2r}{\dot{m}}\sum_{i}^{n}\bar{J}_i\ln(\omega_i)\right] = \exp\left[-\frac{2u_e}{K_* r}\sum_{i}^{n}\bar{J}_i\ln(\omega_i)\right]. \quad (3.1.6b)$$

The drag coefficient at the interval between the $(n-1)$ and (n) states is not determined until the velocity at the (n) state is determined. Thus it is necessary to calculate the drag coefficient using an iterative approach. The term x in equation (3.1.6b) at the ground state or at burn-out state becomes

$$x_o = \exp\left[-\frac{2u_e}{K_* r}\ln\left(\frac{m_o}{m_o}\right)\right] = 1, \quad (3.1.7a)$$
$$x_b = \exp\left[-\frac{2u_e}{K_* r}\sum_{i=1}^{b}\bar{J}_i\ln(\omega_i)\right]. \quad (3.1.7b)$$

The flight time can be represented as a function of the mass.

$$t = \frac{m-m_o}{\dot{m}}. \quad (3.1.8)$$

The altitude of a rocket at burn-out state can be obtained using the time integration of the velocity as follows:

$$h_b = \int_o^{t_b} v\,dt = \frac{1}{\dot{m}}\sum_{i=1}^{b}\int_{m_{i-1}}^{m_i} r\frac{x-1}{x+1}dm. \quad (3.1.9)$$

The above integral cannot be obtained analytically, and thus should be calculated numerically. In the present study, numerical integration using Simpson's rule [29] is applied to obtain the altitude.

3.1.2. Solution in coast phase

In coast phase, the governing equation cannot be integrated analytically since the drag coefficient is not constant. Hence we also have to apply the divide-and-conquer strategy. The differential of the altitude between the $(n-1)$ and (n) states can be expressed as follows:

$$dh = -m_b\frac{v\,dv}{m_b\bar{g}_n + \bar{K}_n v^2}, \quad (3.1.10a)$$
$$\bar{z}_n = \frac{z_{n-1}+z_n}{2}, \quad z = g, K. \quad (3.1.10b)$$

Integrating this equation between the $(n-1)$ and (n) states yields

$$h_n - h_{n-1} = -\frac{m_b}{2}\frac{1}{\bar{K}_n}\ln\left(m_b\bar{g}_n + \bar{K}_n v^2\right)_{v_{n-1}}^{v_n}$$
$$= \frac{m_b}{2}\frac{1}{\bar{K}_n}\ln\left(\frac{m_b\bar{g}_n + \bar{K}_n v_{n-1}^2}{m_b\bar{g}_n + \bar{K}_n v_n^2}\right). \quad (3.1.11a)$$

Then the altitude change from the burn-out state to the stationary state becomes

$$h_{bs} = h_s - h_b = \frac{m_b}{2}\sum_{i=b+1}^{s}\frac{1}{\bar{K}_i}\ln\left(\frac{G_{b,i}+v_{i-1}^2}{G_{b,i}+v_i^2}\right), \quad (3.1.11b)$$
$$G_{b,i} = \frac{m_b\bar{g}_i}{\bar{K}_i}. \quad (3.1.11c)$$

3.2. Optimal condition at burn-out state

The rocket altitude changes with the control parameter, since the rocket velocity also changes with the control parameter. Now, we discuss a way to determine the optimal control parameter for maximizing the altitude at burn-out state. The governing equation (2.6a) can be rewritten according to the altitude instead of the time as follows:

$$\frac{dv}{r^2-v^2} = \frac{J}{m}\frac{dh}{v}. \quad (3.2.1a)$$

Separating the variables and integrating the above equation from ground state to burn-out state yields

$$\int_o^{v_b}\frac{v\,dv}{r^2-v^2} = \int_o^{h_b}\frac{J}{m}dh. \quad (3.2.1b)$$

The left hand side of the above equation is then reduced to

$$-\frac{1}{2}\ln\left(r^2-v^2\right)_o^{v_b} = -\frac{1}{2}\ln\left(1-\frac{v_b^2}{r^2}\right) = -\frac{1}{2}\ln\left[\frac{4x_b}{(x_b+1)^2}\right]. \quad (3.2.2a)$$

Differentiating this term with respect to the control parameter yields

$$\left(-\frac{1}{2x_b}+\frac{1}{x_b+1}\right)\frac{dx_b}{dr} = \frac{1}{2x_b}\frac{x_b-1}{x_b+1}\frac{dx_b}{dr}. \quad (3.2.2b)$$

Differentiating the right hand side of equation (3.2.1b) with respect to the control parameter yields

$$\frac{d}{dr}\int_o^{h_b}\frac{J}{m}dh=\int_o^{h_b}\frac{d}{dr}\frac{J}{m}dh+\frac{J_b}{m_b}\frac{dh_b}{dr}-\frac{J_o}{m_o}\frac{dh_o}{dr}. \tag{3.2.3}$$

The Leibniz rule [30] that prescribes the process to differentiate a definite integral over a variable range is applied in the above equation. The derivative of the altitude at ground state is zero. Also, for the maximum altitude, the derivative of the altitude at burn-out state should be zero. Thus the following characteristic equation must be satisfied for the maximum altitude at burn-out state.

$$\frac{1}{2x_b}\frac{x_b-1}{x_b+1}\frac{dx_b}{dr}=\int_o^{h_b}\frac{d}{dr}\frac{J}{m}dh. \tag{3.2.4}$$

Taking the logarithm of the term x_b in equation (3.1.7b) yields

$$\ln(x_b)=-\frac{2u_e}{K_*r}\sum_{i=1}^{b}\bar{J}_i\ln(\omega_i). \tag{3.2.5a}$$

Then differentiating this equation with respect to the control parameter yields

$$\frac{1}{x_b}\frac{dx_b}{dr}=-\frac{1}{r}\left[\ln(x_b)+\frac{2u_e}{K_*}\sum_{i=1}^{b}\ln(\omega_i)\frac{d\bar{J}_i}{dr}\right]. \tag{3.2.5b}$$

The derivative of the parameter J with respect to the control parameter can be expressed as

$$\frac{dJ}{dr}=\frac{K}{(r^2-v^2)^2}\left[\left(2r\frac{K_*}{K}\left(1+\frac{p_e-p_a}{\rho_e u_e^2}\right)-2v\frac{dv}{dr}\right)(r^2-v^2)-\left(q^2-v^2\right)\left(2r-2v\frac{dv}{dr}\right)\right]. \tag{3.2.5c}$$

Since the derivative of the term $(x-1)/(x+1)$ in equation (3.1.6a) with respect to the control parameter is relatively small, we assume that the term is constant. Then the derivative of the parameter J with respect to the control parameter between the $(n-1)$ and (n) states can be reduced to

$$\frac{d\bar{J}_n}{dr}=\frac{\varphi_n}{2r}, \tag{3.2.5d}$$

$$\varphi_n=\frac{1}{\bar{x}_n}\left[K_*\left(1+\frac{1-p_a/p_e}{\gamma M_e^2}\right)(\bar{x}_n+1)^2-\bar{K}_n(\bar{x}_n-1)^2-4\bar{J}_n\bar{x}_n\right]. \tag{3.2.5e}$$

The drag coefficient changes with the control parameter due to the change in the altitude. However, at the maximum altitude, the derivative of the altitude becomes zero and thus we can ignore the derivative of the drag coefficient. Then equation (3.2.5b) can be reduced to

$$\frac{1}{x_b}\frac{dx_b}{dr}=-\frac{1}{r}\left[\ln(x_b)+\frac{1}{r}\frac{u_e}{K_*}\sum_{i=1}^{b}\ln(\omega_i)\varphi_i\right]. \tag{3.2.5f}$$

The rocket mass at a given altitude can be expressed as a function of the time and the control parameter.

$$m=m(t,r). \tag{3.2.6a}$$

The derivative of the mass with respect to the control parameter becomes

$$\frac{dm}{dr}=\left(\frac{\partial m}{\partial t}\right)_r\frac{dt}{dr}+\left(\frac{\partial m}{\partial r}\right)_t. \tag{3.2.6b}$$

The partial derivative of the mass with respect to the control parameter is

$$\frac{\partial m}{\partial r}=t\frac{d\dot{m}}{dr}=\frac{m-m_o}{\dot{m}}\frac{d}{dr}\frac{K_*r^2}{u_e}=\frac{2K_*r(m-m_o)}{\dot{m}u_e}=\frac{2(m-m_o)}{r}. \tag{3.2.6c}$$

The derivative of the time with respect to the control parameter contains the derivative of the mass with respect to the control parameter. Thus, equation (3.2.6b) is trivial and does not give an explicit expression of the derivative of the mass with respect to the control parameter. As suggested in previous studies [22,23], the derivative of the mass with respect to the control parameter can be expressed as follows:

$$\frac{dm}{dr}=\frac{2(m-\beta m_b)}{r}. \tag{3.2.6d}$$

The parameter β in equation (3.2.6d) could be interpreted as a balancing weight. Since the rocket mass at a given altitude changes with the mass flow rate, the derivative of the mass with respect to the control parameter is dependent on the mass flow rate. Therefore, the coefficient β could be determined to satisfy the optimal condition for maximizing altitude.

The right hand side of equation (3.2.4) then becomes

$$\int_o^{h_b}\frac{d}{dr}\frac{J}{m}dh=\int_o^{h_b}-\frac{J}{m^2}\frac{dm}{dr}+\frac{1}{m}\frac{dJ}{dr}dh=-\frac{1}{r}\sum_{i=1}^{b}\int_{h_{i-1}}^{h_i}\frac{1}{m}\left[2\bar{J}_i\left(1-\beta\frac{m_b}{m}\right)-\frac{1}{2}\varphi_i\right]dh. \tag{3.2.6e}$$

Hence, the following characteristic equations should be satisfied to maximize the altitude at burn-out state.

$$r=-\frac{u_e}{K_*}\frac{L_b}{\ln(x_b)-S_b}, \tag{3.2.7a}$$

$$L_b=\sum_{i=1}^{b}\ln(\omega_i)\varphi_i, \tag{3.2.7b}$$

$$S_b=\frac{x_b+1}{x_b-1}\sum_{i=1}^{b}\int_{h_{i-1}}^{h_i}\frac{1}{m}\left[4\bar{J}_i\left(1-\beta\frac{m_b}{m}\right)-\varphi_i\right]dh. \tag{3.2.7c}$$

The solution of the characteristic equation cannot be obtained analytically since the undetermined solution exists implicitly. Thus, we try to obtain the solution using an iterative solution method. The iterative procedure is very sensitive to the control parameter and the parameter β. When the rocket mass ratio is high, a serious numerical instability might occur. Hence we introduce an ad-hoc to relax the sensitivity of the characteristic equation (3.2.7) with dispersing the side effects. We introduce the stabilizer λ to relax numerical instabilities that might occur during iterative calculations.

$$r_{k+1}=\frac{u_e}{K_{*,k}}\frac{L_{b,k}}{\ln(x_{b,k})-S_{b,k}}, \tag{3.2.8a}$$

$$L_{b,k}=\left\{\sum_{i=1}^{b}\ln(\omega_i)\varphi_i\right\}_k, \tag{3.2.8b}$$

$$S_{b,k}=\left\{\lambda\frac{x_b+1}{x_b-1}\sum_{i=1}^{b}\int_{h_{i-1}}^{h_i}\frac{1}{m}\left[4\bar{J}_i\left(1-\beta\frac{m_b}{m}\right)-\varphi_i\right]dh\right\}_k. \tag{3.2.8c}$$

The stabilizer would be a function of the parameter β, since the stabilizer λ in the above equation introduced to disperse the side effects from the variation of the parameter β. A preliminary numerical experiment shows that the following function works well.

$$\lambda_k = \frac{1}{2} + \beta_k. \tag{3.2.8d}$$

The initial guess of the control parameter should guarantee that the thrust be larger than the gravitational force at ground state. We take the following initial guess.

$$r_0 = \sqrt{2\frac{m_o g_o - A_e(p_e - p_o)}{C_K K_o}}. \tag{3.2.8e}$$

The coefficient C_K is determined by experience to ensure the initial guess of the control parameter in equation (3.2.8e) sufficiently high. A preliminary numerical experiment shows that the coefficient C_K of 0.01 guarantees stable convergence up to a mass ratio of 6.

After updating the control parameter, the mass flow rate and the critical drag coefficient K_* should be updated. During the updating procedure of the critical drag coefficient the mass flow rate should be kept unchanged. Thus the control parameter should be adjusted to maintain the consistency of the relation. Hence the updating procedure should be conducted in the following order.

$$(1)\ \dot{m}_{k+1} = \frac{K_{*,k} r_{k+1,temp}^2}{u_e}, \tag{3.2.9a}$$

$$(2)\ K_{*,k+1} = \left\{ K_b - \frac{A_e(p_e - p_{a,b}) - m_b g_b}{r^2} \right\}_{k+1}, \tag{3.2.9b}$$

$$(3)\ r_{k+1} = \sqrt{\frac{\dot{m}_{k+1} u_e}{K_{*,k+1}}}. \tag{3.2.9c}$$

The term $r_{k+1,temp}$ stands for the temporal control parameter calculated by equation (3.2.8a), while the term r_{k+1} does the adjusted control parameter.

As mentioned above right after equation (3.2.6d), if the parameter β is determined to match the optimal condition for maximizing altitude, we could obtain the optimal control parameter. The term S_b in equation (3.2.8c) decreases and thus the estimated control parameter increase as the coefficient β increases. Therefore, we can determine the coefficient β with the following iterative relation as

$$\beta_{k+1} = \beta_k \left[1 - C_\beta \left(\frac{r}{h_b} \frac{dh_b}{dr} \right)_k \right]. \tag{3.2.10a}$$

The coefficient C_β is determined by experience to keep the convergence of the iterative procedure stable by controlling the changing rate of the coefficient β. A large value of the coefficient C_β in the above equation gives fast convergence but would result in serious instabilities. In the present study, the constant of 0.05 is used. In contrast to the cases with a constant drag parameter considered in the previous study [22], the derivative of the altitude with respect to the control parameter cannot be explicitly determined since the drag parameter changes with the altitude, which is not yet determined. A reasonable and simple alternative is the numerical derivative represented as follows:

$$\frac{\partial h_b}{\partial r} \approx \frac{h_b(r + \Delta r) - h_b(r - \Delta r)}{2\Delta r}. \tag{3.2.10b}$$

A small value of the difference in the control parameter Δr gives precise differentiation but would result in serious instabilities. A preliminary numerical experiment shows that the difference in the control parameter Δr between 0.1% and 1.0% of the control parameter guaranteed stable convergences. In the present study, a difference of 0.5% of the control parameter is used.

3.3. Optimal condition at apogee

The rocket in coast phase ascends until apogee. Hence, the optimal condition for maximizing the altitude at apogee would differ from that at burn-out state. In coast phase, the thrust is terminated and the mass is constant. Therefore, the governing equation becomes

$$-\int_{v_b}^{o} \frac{K v dv}{K v^2 + m_b g} = \int_{h_b}^{h_s} \frac{K}{m_b} dh. \tag{3.3.1}$$

Adding the above equation to equation (3.2.1b) yields

$$\int_{o}^{v_b} \frac{v dv}{r^2 - v^2} - \int_{v_b}^{o} \frac{K v dv}{K v^2 + m_b g} = \int_{o}^{h_b} \frac{J}{m} dh + \int_{h_b}^{h_s} \frac{K}{m_b} dh. \tag{3.3.2}$$

The previous study [23] shows the second integral in the left hand side of equation (3.3.2) can be reduced to

$$-\int_{v_b}^{o} \frac{K v dv}{K v^2 + m_b g} = \frac{1}{2 + \psi} \ln\left(\frac{G_{b,b} + v_b^2}{G_{b,b}} \right), \tag{3.3.3a}$$

$$\psi = \frac{\ln[K(v_b)/K(v_b/2)]}{\ln(2)}, \tag{3.3.3b}$$

$$G_{b,b} = \frac{m_b g_b}{K_b}. \tag{3.3.3c}$$

Further, the previous study [23] shows that the derivative of the above term with respect to the control parameter can be reduced to

$$\frac{d}{dr} \frac{1}{2 + \psi} \ln\left(\frac{G_{b,b} + v_b^2}{G_{b,b}} \right) = \frac{2}{2 + \psi} \frac{x_b - 1}{x_b + 1} \frac{r}{G_{b,b} + v_b^2} \left[\frac{x_b - 1}{x_b + 1} + \frac{2r}{(x_b + 1)^2} \frac{dx_b}{dr} \right]. \tag{3.3.3d}$$

Differentiating the right hand side of equation (3.3.2) with respect to the control parameter yields

$$\frac{d}{dr} \left(\int_{o}^{h_b} \frac{J}{m} dh + \int_{h_b}^{h_s} \frac{K}{m_b} dh \right) = \int_{o}^{h_b} \frac{d}{dr} \frac{J}{m} dh + \int_{h_b}^{h_s} \frac{d}{dr} \frac{K}{m_b} dh + \frac{J_b}{m_b} \frac{dh_b}{dr} - \frac{J_o}{m_o} \frac{dh_o}{dr} + \frac{K_s}{m_b} \frac{dh_s}{dr} - \frac{K_b}{m_b} \frac{dh_b}{dr}. \tag{3.3.4}$$

The Leibniz rule [30] is applied. The second and the last terms cancel out. The derivative of the altitude at ground state is zero, and, for the maximum altitude, the derivative of the altitude at apogee should be zero. The rocket mass after burn-out state is constant, and thus its derivative is zero, and the derivative of the drag parameter vanishes. Thus we can ignore the second term. The third term and the last term could cancel out since, as mentioned in equation (3.1.2b), the parameter J becomes the drag parameter K at burn-out state.

Hence, only the first term in equation (3.3.4) remains and the characteristic equation to indicate the optimal condition for maximizing the altitude at apogee becomes

$$\frac{1}{2x_b}\frac{x_b-1}{x_b+1}\frac{dx_b}{dr}+\frac{2}{2+\psi}\frac{x_b-1}{x_b+1}\frac{r}{G_{b,b}+v_b^2}\times\left[\frac{x_b-1}{x_b+1}+\frac{2rx_b}{(x_b+1)^2}\frac{1}{x_b}\frac{dx_b}{dr}\right]=\int_o^{h_b}\frac{d}{dr}\frac{J}{m}dh. \tag{3.3.5a}$$

Rearranging the above equation yields

$$\Gamma_b\frac{1}{x_b}\frac{dx_b}{dr}+\frac{4r}{2+\psi}\frac{x_b-1}{x_b+1}=2\left(G_{b,b}+v_b^2\right)\frac{x_b+1}{x_b-1}\int_o^{h_b}\frac{d}{dr}\frac{J}{m}dh, \tag{3.3.5b}$$

$$\Gamma_b=G_{b,b}+v_b^2+\frac{8r^2}{2+\psi}\frac{x_b}{(x_b+1)^2}. \tag{3.3.5c}$$

Inserting equation (3.2.5f) and equation (3.2.6e) into the above equation yields

$$\left[\ln(x_b)+\frac{1}{r}\frac{u_e}{K_*}L_b\right]\Gamma_b-\frac{4r^2}{2+\psi}\frac{x_b-1}{x_b+1}=\left(G_{b,b}+v_b^2\right)S_b. \tag{3.3.5d}$$

Therefore, the following characteristic equations should be satisfied to maximize the altitude of a rocket at apogee.

$$r=\frac{u_e}{K_*}\frac{L_b}{\ln(x_b)-S_s}, \tag{3.3.6a}$$

$$L_b=\sum_{i=1}^{b}\ln(\omega_i)\varphi_i, \tag{3.3.6b}$$

$$S_s=\frac{4r^2}{\Gamma_b(2+\psi)}\frac{x_b-1}{x_b+1}+\frac{G_{b,b}+v_b^2}{\Gamma_b}\frac{x_b+1}{x_b-1}\times\sum_{i=1}^{b}\int_{h_{i-1}}^{h_i}\frac{1}{m}\left[4\bar{J}_i\left(1-\beta\frac{m_b}{m}\right)-\varphi_i\right]dh. \tag{3.3.6c}$$

The solution of the characteristic equation cannot be obtained analytically since the undetermined solution exists implicitly in the second term. Thus, we try to obtain the solution using the following iterative solution method. As mentioned in the above section, the iterative procedure is very sensitive to the control parameter and the parameter β. Thus we introduce a stabilizer λ.

$$r_{k+1}=\frac{u_e}{K_{*,k}}\frac{L_{b,k}}{\ln(x_{b,k})-S_{s,k}}, \tag{3.3.7a}$$

$$L_{b,k}=\left\{\sum_{i=1}^{b}\ln(\omega_i)\varphi_i\right\}_k, \tag{3.3.7b}$$

$$S_{s,k}=\left\{\frac{4r^2}{\lambda\Gamma_b(2+\psi)}\frac{x_b-1}{x_b+1}+\lambda\frac{G_{b,b}+v_b^2}{\Gamma_b}\frac{x_b+1}{x_b-1}\times\sum_{i=1}^{b}\int_{h_{i-1}}^{h_i}\frac{1}{m}\left[4\bar{J}_i\left(1-\beta\frac{m_b}{m}\right)-\varphi_i\right]dh\right\}_k, \tag{3.3.7c}$$

$$\Gamma_{b,k}=\left\{G_{b,b}+v_b^2+\lambda\frac{8r^2}{2+\psi}\frac{x_b}{(x_b+1)^2}\right\}_k, \tag{3.3.7d}$$

$$\lambda_k=\frac{1}{2}+\beta_k. \tag{3.3.7e}$$

If the optimal condition at burn-out state is known, we can easily determine the initial value of the control parameter as follows:

$$r_0=\sqrt{2\frac{m_o g_o-A_e(p_e-p_o)}{K_{b,optb}}}. \tag{3.3.7f}$$

The updating procedure of the mass flow rate and the critical drag parameter at the $(k+1)$ step and the adjustment of the control parameter are the same as those in equations (3.2.9a)–(3.2.9c).

The term $S_{s,k}$ in equation (3.3.7c) decreases and thus the estimated control parameter r_{k+1} increases as the coefficient β increases. Therefore, we can determine the coefficient β with the following iterative relation.

$$\beta_{k+1}=\beta_k\left[1-C_\beta\left(\frac{r}{h_s}\frac{dh_s}{dr}\right)_k\right]. \tag{3.3.8a}$$

As mentioned in section 3.2, the derivative of the altitude with respect to the control parameter could not be explicitly determined since the drag parameter changes with the altitude, which is not yet determined. A reasonable and simple alternative is the numerical derivative represented as follows:

$$\frac{\partial h_s}{\partial r}\approx\frac{h_s(r+\Delta r)-h_s(r-\Delta r)}{2\Delta r}. \tag{3.3.8b}$$

A large value of the coefficient C_β in equation (3.2.9a) gives fast convergence but would result in serious instabilities. In the present study, the constant 0.05 is used. On the other hand, a small value in the difference of the control parameter Δr gives precise differentiation but would result in serious instabilities. Preliminary numerical experiments showed that a difference in the control parameter Δr between 0.1% and 1.0% of the control parameter guaranteed stable convergence. In the present study, a difference of 0.5% of in control parameter is adopted.

4. Numerical solutions

If the mass and the rocket velocity are known at the $(n-1)$ state, then the velocity at the (n) state can be numerically obtained. The discretized governing equation of the rocket motion in boost phase becomes

$$\bar{m}_n\frac{v_n-v_{n-1}}{\Delta t}=\bar{F}_{e,n}-\bar{K}_n\bar{v}_n^2-\bar{m}_n\bar{g}_n, \tag{4.1a}$$

$$\bar{F}_{e,n}=\dot{m}u_e+A_e(p_e-\bar{p}_{a,n}), \tag{4.1b}$$

$$\Delta t=t_n-t_{n-1}=\frac{m_n-m_{n-1}}{\dot{m}}. \tag{4.1c}$$

The over-bar denotes the average of the variable between the $(n-1)$ and (n) states.

$$\bar{z}_n=\frac{z_{n-1}+z_n}{2},\qquad z=m,\,v,\,g,\,p_a,\,K. \tag{4.1d}$$

The governing equation is then rewritten as follows:

$$\bar{m}_n\frac{v_n-v_{n-1}}{\Delta t}=\bar{F}_{e,n}-\frac{\bar{K}_n}{4}\left(v_{n-1}^2+2v_{n-1}v_n+v_n^2\right)-\bar{m}_n\bar{g}_n. \tag{4.2a}$$

This discretized equation becomes quadratic, as follows:

$$v_n^2+2\left(v_{n-1}+2\frac{\bar{m}_n}{\bar{K}_n\Delta t}\right)v_n+v_{n-1}^2-\frac{4}{\bar{K}_n}\left(\bar{m}_n\frac{v_{n-1}}{\Delta t}+\bar{F}_{e,n}-\bar{m}_n\bar{g}_n\right)=0. \tag{4.2b}$$

The solution of the above equation at the (n) state is

$$v_n=-B+\sqrt{B^2-C}, \tag{4.3a}$$

$$B=v_{n-1}+2\frac{\bar{m}_n}{\bar{K}_n\Delta t},$$

$$C=v_{n-1}^2-\frac{4}{\bar{K}_n}\left(\bar{m}_n\frac{v_{n-1}}{\Delta t}+\bar{F}_{e,n}-\bar{m}_n\bar{g}_n\right). \tag{4.3b}$$

The discretized governing equation of the rocket motion in coast can be constructed if the thrust term is extracted and the mass is fixed as that at the burn-out state.

$$v_n = -B + \sqrt{B^2 - C}, \tag{4.4a}$$

$$B = v_{n-1} + 2\frac{m_b}{\bar{K}_n \Delta t}, \qquad C = v_{n-1}^2 - \frac{4}{\bar{K}_n}\left(m_b \frac{v_{n-1}}{\Delta t} - m_b \bar{g}_n\right). \tag{4.4b}$$

5. Calculation conditions

5.1. Atmosphere

The solution of the rocket equation depends strongly on the drag coefficient, which varies with the ambient air density. Therefore, for the flight of a rocket in a real atmosphere, the density change with the altitude raises a critical issue for rocket dynamics. In the present study, the density is determined according to the US standard atmosphere [24] where the effects of wind, location or time are excluded. The standard atmosphere is composed of the troposphere, stratosphere, mesosphere, and thermosphere.

The temperature at an altitude between the adjacent layers is obtained with a linear interpolation. The pressure in each interval is expressed as an exponential function of the altitude. Then the pressure at an altitude between the adjacent layers is obtained with an exponential interpolation. We can then determine the density as a function of the altitude with the thermodynamic state function for the ideal gas of air. For detail, refer to the article [23].

5.2. Aerodynamic drag coefficient

The cross-sectional diameter of the rocket is 0.6 m. The aerodynamic drag coefficient C_d is not a constant but is instead a function of the Mach number. The basic model used to simulate the effect of the Mach number is the one used by Ganji [21]. However the basic model showed some unstable behavior near the Mach number of one. Hence, in the present study, the following model [23], which is modified to have smooth transitions near the Mach number of one, is adopted.

$$C_d = C_{do}\left[1 + R_d f_d(M)\right], \tag{5.1a}$$

$$f_d(M) = \begin{cases} A_0 M^4, & M \le 1 \\ 1 - A_1(M - M_1)^4, & 1 < M \le M_2 \\ A_2(M + 1 - M_2)^{-1} & M_2 < M \end{cases}, \tag{5.1b}$$

$$A_1 = \frac{1 - A_0}{(M_1 - 1)^4}, \qquad A_2 = 1 - A_1(M_2 - M_1)^4. \tag{5.1c}$$

The aerodynamic drag coefficient at ground state C_{do} and the jump ratio of the drag coefficient R_d are set as 0.8 and 1.1, respectively. The Mach numbers M_1 and M_2 in the above equation are set as 1.2 and 1.325, respectively. The coefficient A_0 is fixed as 0.75. These coefficient A_0 and Mach numbers M_1 and M_2 are determined arbitrary to make smooth change of the drag coefficient.

5.3. Rocket launching conditions

In the present study, a rocket dry-mass of 750 kg is considered. Rocket dry-masses of 500 kg and 1000 kg are also considered for comparisons. The total mass or the propellant mass is determined according to the mass ratio Ω. The mass ratio is varied from 2 to 6, which means the rocket total mass is changed from 1500 kg to 4500 kg.

We consider the launching conditions of KSR III. The combustor temperature and pressure are fixed as 2500 K and 750 kPa, respectively. The Mach number at the nozzle exit is determined by considering the jet pressure at the nozzle exit to be larger than the one third of the ambient pressure at ground state to prevent flow separation at the nozzle exit. Therefore, in the present study, the Mach number at nozzle exit is fixed as 4.0. The specific heat ratio is fixed as 1.27. Then the temperature and the pressure at the nozzle exit are determined by the isentropic equations (2.3a) and (2.3b) as 791.1 K and 33.47 kPa, respectively. The jet velocity at the nozzle exit is determined by equation (2.3c) as 2148 m/s.

The mass flow rate of propellant changes according to the control parameter and thus is determined with equation (3.1.2a) if the control parameter is determined. The nozzle throat area is determined according to the mass flow rate with equation (2.2c). Then the nozzle exit area is determined by equation (2.3d).

5.4. Numerical calculations

If the number of piecewise intervals increases, the numerical solution or the piecewise analytic solution becomes more exact. A preliminary numerical experiment shows that in case the number of intervals for boost phase is as high as 150, then numerical integration with the trapezoid rule yields almost the same result as that with Simpson's rule [29]. The number of piecewise intervals for boost phase and coast phase are both fixed as 400. The mass change during each interval is assumed to be constant.

$$m_n - m_{n-1} = \frac{m_b - m_o}{N_b} = const. \tag{5.2}$$

During the calculations of equation (3.2.8) or (3.3.7), three key parameters are updated: the control parameter r, the coefficient β and the critical drag parameter K_*. Simultaneous changes in the key parameters could cause serious numerical instabilities. If we calculate the coefficient β_{k+1} in equation (3.2.10) or (3.3.8) with the newly updated control parameter r_{k+1}, we could encounter a serious numerical instability.

Sometimes, an abrupt numerical instability might occur during iterative calculations, which is usually due to the situation where the temporary calculated control parameter is too small and thus the thrust is smaller than the gravitational force. In this case, we should make sure that the thrust is larger than the gravitational force and calculate the characteristic equations with a smaller coefficient C_β in equation (3.2.10) or (3.3.8).

6. Results

6.1. Solution profiles

Fig. 1 compares the velocity profiles between the pseudo-analytic and the numerical solutions. The vertical dashed line indicates the burn-out time. The rocket velocities increase steeply from ground state and furthermore the accelerations grow due to the reduction of the rocket mass until burn-out state. In coast phase, the velocities decrease due to the gravity force and aerodynamic drag. Fig. 1a shows the variations in the velocity profile according to the rocket mass ratio with a fixed rocket mass of 750 kg. Regardless of the rocket mass ratio, each pseudo-analytic solution is identical to the numerical one. The case with a higher mass ratio yields a higher rocket velocity and a longer time to apogee. Fig. 1b shows the variation in the velocity profiles based on the rocket mass with a fixed rocket mass ratio of 4. Regardless of the rocket mass, each pseudo-analytic solution is identical to the numerical one. The case with a higher mass yields a slight higher velocity but a similar time to apogee.

Fig. 2 shows the changes in the altitude with time. The vertical dashed line indicates the burn-out time. In boost phase, the rocket altitude increases through a concave curve due to the increasing velocity until burn-out state. In coast phase, the rocket altitude

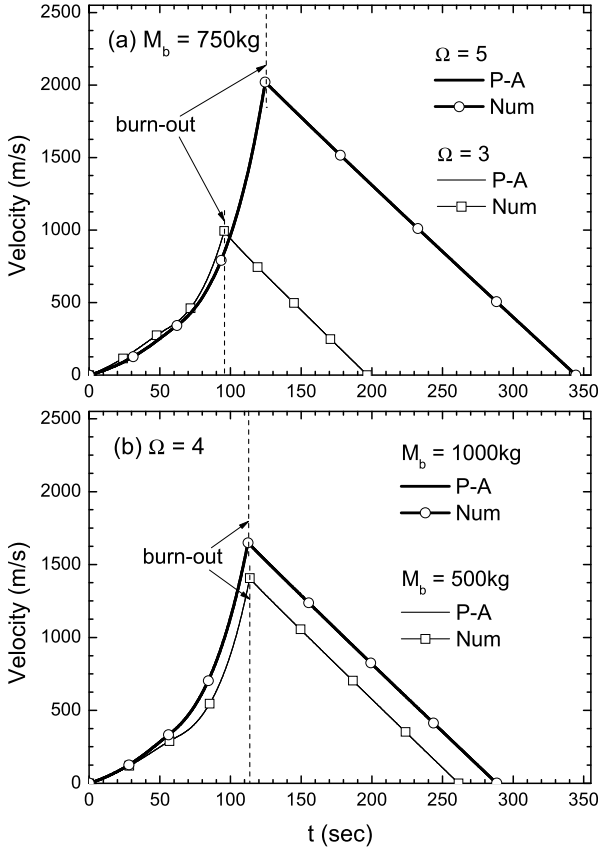

Fig. 1. Velocity profile as a function of time.

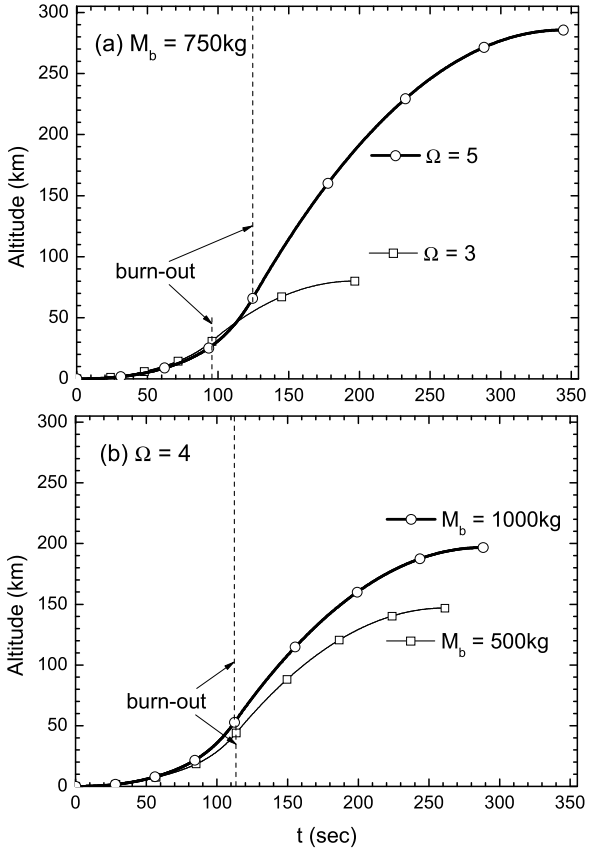

Fig. 2. Changes in altitude as a function of time.

changes through a convex curve, since the rocket is decelerated by gravity.

Fig. 2a shows the variations in the altitude as a function of the rocket mass ratio with a fixed rocket mass of 750 kg. The increase in the rocket mass ratio results in an increase in the maximum altitude. Fig. 2b shows the variation of the altitude according to the rocket mass with a fixed rocket mass ratio of 4. The case with a higher mass yields a higher altitude but a similar time to apogee.

6.2. Optimal conditions at burn-out state

To estimate the characteristic changes in the altitude at burn-out state according to the control parameter, the normalized control parameter and the normalized altitude at burn-out state are introduced as follows:

$$\phi_b = \frac{r - r_{opt,b}}{r_{opt,b}}, \tag{6.1a}$$

$$\eta_b = \frac{h_b}{h_b(r_{opt,b})}. \tag{6.1b}$$

Fig. 3 shows variations in the altitude at burn-out state according to the control parameter. The vertical dashed lines indicate the normalized optimal control parameter calculated by equation (3.2.8). The characteristic equation gives exact predictions of the optimal control parameter regardless of the rocket masses or mass ratios. The mass flow rates in the figures represent the optimal values at burn-out state. Fig. 3a represents the effects of the mass ratio on the rocket altitude. The case with a mass ratio of 2 seems much less sensitive to the control parameter than the other cases. Fig. 3b represents the effects of the rocket mass on the rocket altitude. The normalized curves with different rocket masses nearly coincide even though the difference in the rocket

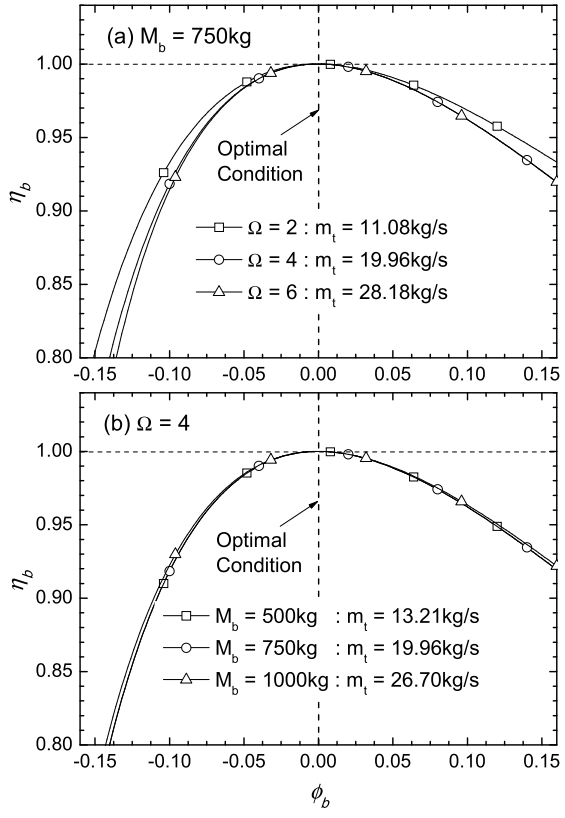

Fig. 3. Variation in altitude at burn-out state as a function of the control parameter.

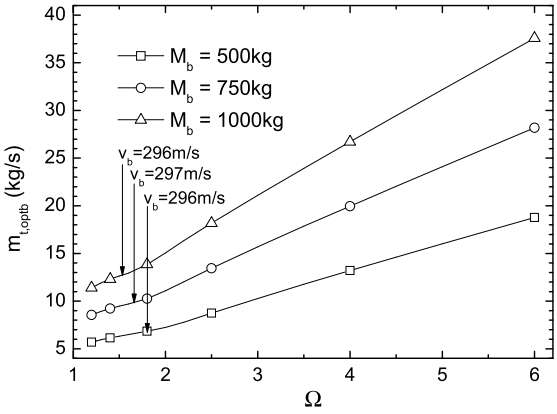

Fig. 4. Variation in optimal mass flow rate at burn-out state.

mass is large. This suggests that the variation in the normalized altitude is largely insensitive to the rocket mass. From equation (3.1.2a), we can deduce the relation: $d\dot{m}/\dot{m} = 2dr/r$, which implies that the same relative change of the control parameter results in the same relative change of the thrust. As shown in Fig. 3b, the ratios between the rocket mass and the mass flow rate are almost same with each other. Hence, if we neglect the effects of the aerodynamic drag, the same changes of the relative control parameter (ϕ_b) result in the same changes of acceleration. This may be the reason why the curves coincide.

Fig. 4 shows variations in the optimal mass flow rate with the rocket mass or the rocket mass ratio at burn-out state. For a given rocket mass ratio, the optimal mass flow rate grows with the rocket mass but the growth rate slightly decreases as the rocket mass increases.

For a given mass, there are two regions where the increasing rates of the optimal mass flow rate are slightly different. There are also slight concave regions where the rocket mass ratio is between 1.5 and 2.5. In that region, the rocket velocities at burn-out state are near to the speed of sound where the aerodynamic drag coefficient sharply changes. This might be the reason why there exist the inversions of the concavities. After the inversion of the concavity, the optimal mass flow rate increases in a linear mode, since the flight Mach number is much higher than unity and the rocket flies in a rarefied air for a relatively long time.

Fig. 5 shows variations in the maximum altitude at burn-out state with the rocket mass or the rocket mass ratio for the optimal mass flow rate at burn-out state. The velocities shown the figure are the velocities at burn-out state when the rocket dry-mass is 750 kg. For a given rocket mass ratio, the maximum altitude increases with the rocket mass but the rate slightly decreases as the rocket mass increases. For a given rocket mass, the altitude at burn-out state grows with the mass ratio in a linear mode at low mass ratios and along a convex line at high mass ratios. The convex curve of the altitude at burn-out state at high mass ratios is due to the fact that the rocket at a higher velocity suffers a higher aerodynamic drag. The altitude at apogee grows with the mass ratio along a concave line until the mass ratio becomes 3.5 and there it grows with the mass ratio in a linear fashion.

6.3. Optimal conditions at stationary state

To determine the characteristic changes of the altitude at stationary state or apogee according to the control parameter, the normalized control parameter and the normalized altitude at apogee are introduced as follows:

$$\phi_s = \frac{r - r_{opt,s}}{r_{opt,s}}, \tag{6.2a}$$

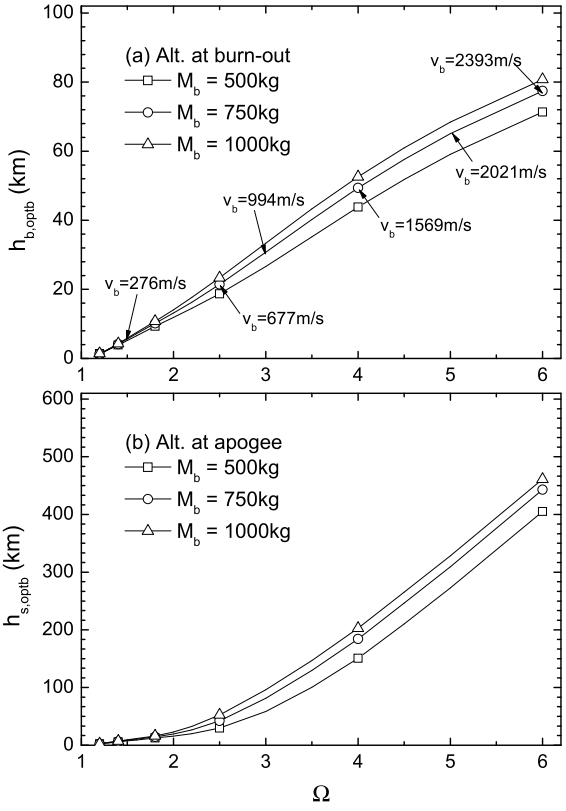

Fig. 5. Variations in maximum altitude at burn-out state and at apogee.

$$\eta_s = \frac{h_s}{h_s(r_{opt,s})}. \tag{6.2b}$$

Fig. 6 shows variations in the altitude at apogee according to the control parameter. The vertical dashed line indicates the normalized optimal control parameter calculated by the characteristic equation (3.3.7). The characteristic equation gives exact predictions of the optimal control parameter regardless of the rocket masses or mass ratios. The values of the control parameter in the figures represent the optimal ones at apogee. Fig. 6a represents the effects of the mass ratio on the altitude. The case with a lower mass ratio is much more sensitive to the control parameter. Fig. 6b represents the effects of the rocket mass on the altitude. Again, the case with a lower mass ratio is much more sensitive to the control parameter, which is different from the optimal cases at burn-out state.

Fig. 7 shows the variations in the optimal mass flow rate with the rocket mass and the rocket mass ratio at apogee. For a given rocket mass ratio, the optimal mass flow grows with the rocket mass. The optimal mass flow for a given rocket mass decreases sharply with the mass ratio until a minimum value where the mass ratio is near 1.5 and, after the point, the mass flow turns around and grows gradually, which is very different behavior from the situation at burn-out state shown in Fig. 4. These characteristic changes look similar to those shown in the previous study [23]. After the concave region, the optimal mass flow rate increases in a linear mode, since the flight Mach number is much higher than unity and the rocket flies in a rarefied air for a relatively long time.

Fig. 8 shows variations in the maximum altitude at apogee with the rocket mass and the rocket mass ratio for the optimal mass flow rate at apogee. The velocities shown the figure are the velocities at burn-out state when the rocket dry-mass is 750 kg.

In contrast to the case for the optimal condition at burn-out state, the maximum altitudes for a given rocket mass ratio are nearly identical, regardless of the rocket mass or the rocket mass

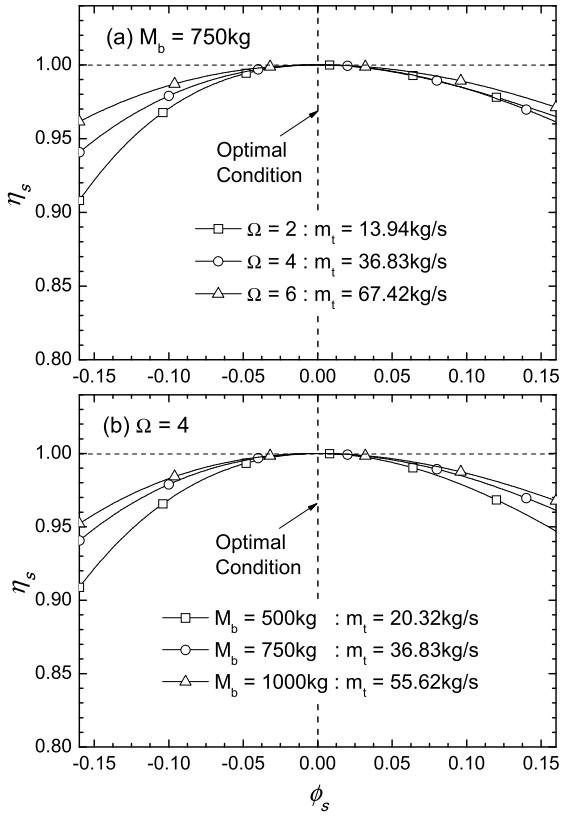

Fig. 6. Variation in altitude at apogee as a function of the control parameter.

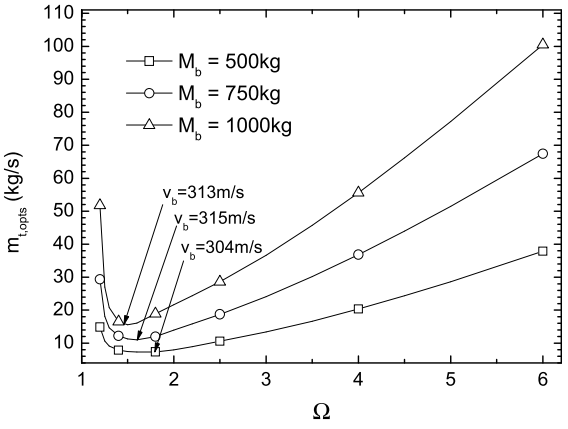

Fig. 7. Variation in optimal mass flow rate at apogee.

ratio. For a given rocket mass ratio, the maximum altitude at apogee increases with the rocket mass but the rate slightly decreases as the rocket mass increases. For a given rocket mass, the altitude growth rate increases until the mass ratio becomes 3.5, and after the altitude grows linearly with the mass ratio. The final altitude for the optimal condition at apogee is much higher than that for the optimal condition at burn-out state. The linear increase of the altitude at apogee with the mass ratio is due to the fact that the rocket flies through the coast phase for a relatively long time in a rarefied air where the aerodynamic drag is very weak.

7. Conclusions

The one-dimensional rocket momentum equation including thrust, gravitational force, and aerodynamic drag is examined to pseudo-analytically determine the optimal condition for maximizing the altitude of a sounding rocket at burn-out state or at apogee. The analytic approach for determining the optimal conditions for maximizing the altitude of a sounding rocket flying in a standard atmosphere is extended to the case in which the mass flow rate of propellant is constant. If the mass flow rate is constant, we could not obtain an analytic solution of the governing equation. Hence we introduce a new pseudo-analytic approach to overcome these difficulties. The rocket flights in a standard atmosphere where the air density as well as the gravitational acceleration change with the altitude are considered. In addition, the change in the aerodynamic drag coefficient with the Mach number is considered. The piecewise pseudo-analytic solutions are obtained with a divide-and-conquer strategy with which the entire flight time is divided into small intervals where the drag parameter and the gravitational acceleration can be treated as constants in each interval.

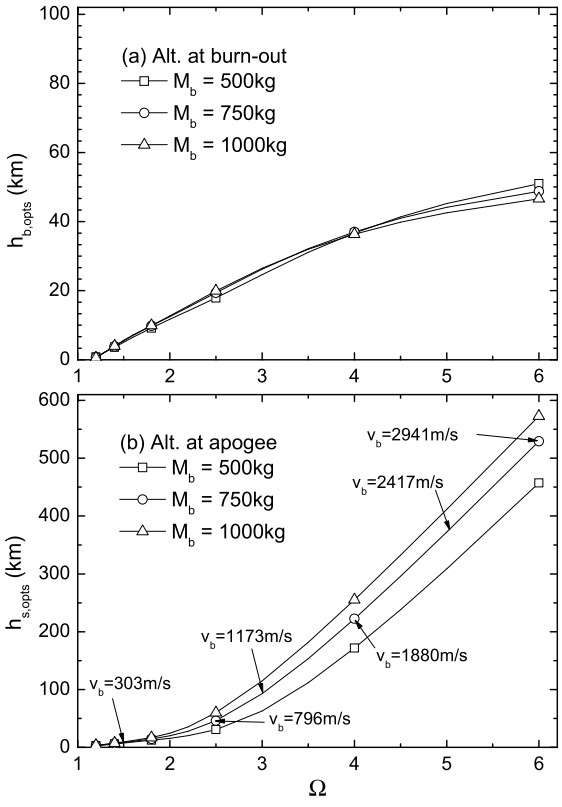

Fig. 8. Variations in maximum altitude at burn-out state and at apogee.

A piecewise pseudo-analytic rocket velocity for a given control parameter can be obtained that matches the numerical one. For a given launching condition, there exists an optimal control parameter corresponding to the optimal mass flow rate of propellant for maximizing the altitude at burn-out state or at apogee. A pseudo-analytic characteristic equation constructed from the pseudo-analytic solution of the governing equation provides accurate predictions of the optimal conditions for maximizing the altitude at burn-out state or apogee, which is confirmed by the numerical experiments.

In a burn-out situation, the increase in the rocket mass at a given mass ratio results in the increases in the optimal mass flow rate, but the increasing rate decreases as the rocket mass increases. The optimal mass flow rate at a given rocket mass grows with the rocket mass ratio in a linear mode. In an apogee situation, the optimal mass flow rate for maximizing the altitude at apogee exists and is higher than that at the burn-out situation. Like the situation at burn-out state, the optimal mass flow rate grows with the rocket mass, but there is a mass ratio where the optimal mass flow rate shows a minimum. This occurs where the mass ratio is near

1.5 at a given rocket mass, which is not shown in the burn-out situation.

Conflict of interest statement

There is no conflict of interest.

Acknowledgements

This study was supported by a Research Fund of the University of Ulsan.

References

[1] S.F. Singer, Research in the upper atmosphere with high altitude sounding rockets, Vistas Astron. 2 (1) (1956) 878–912.
[2] G. Alford, G. Cooper, N. Peterson, Sounding rockets in Antarctica, in: 6th Sounding Rocket Conference, AIAA 1982-1754.
[3] M. Sanchez-Pena, Scientific experiences using Argentinean sounding rockets in Antarctica, Acta Astronaut. 47 (2000) 301–307.
[4] J.M. Grebowsky, D. Bilitza, Sounding rocket data base of E and D region ion composition, Adv. Space Res. 25 (1) (2000) 183–192.
[5] C.L. Croskey, J.D. Mitchell, M. Friedrich, K.M. Torkar, R.A. Goldberg, Charged particle measurements in the polar summer mesosphere obtained by DROPPS sounding rockets, Adv. Space Res. 28 (7) (2001) 1047–1052.
[6] S. Nakasuka, R. Funase, K. Nakada, N. Kaya, J.C. Mankins, Large membrane Furoshiki Satellite applied to phased array antenna and its sounding rocket experiment, Acta Astronaut. 58 (2006) 395–400.
[7] K. Dougherty, Upper atmospheric research at Woomera: the Australian-built sounding rockets, Acta Astronaut. 59 (2006) 54–67.
[8] G-R. Cho, J-J. Park, E-S. Chung, S-H. Hwang, The Korea sounding rocket program, Acta Astronaut. 62 (2008) 706–714.
[9] P.J. Eberspeaker, D.D. Gregory, An overview of the NASA sounding rocket and balloon programs, in: 19th ESA Symposium on European Rocket and Balloon Programmes and Related Research, Bad Reichenhall, Germany, 7–11 June 2009.
[10] P. Sanz-Aranguez, J.S. Calero, Sounding rocket developments in Spain, Acta Astronaut. 64 (2009) 850–863.
[11] J-S. Chern, B. Wu, Y-S. Chen, A-M. Wu, Suborbital and low-thermospheric experiments using sounding rockets in Taiwan, Acta Astronaut. 70 (2012) 159–164.
[12] J.M.C. Romero, Sounding rocket program in Peru, SpaceOps 2012 Conference, 2012-1275893.
[13] P.R. Richter, M. Lebert, H. Tahedl, D-P. Hader, Physiological characterization of gravitaxis in Euglena gracilis and Astasia longa studies on sounding rocket flights, Adv. Space Res. 27 (5) (2001) 983–988.
[14] T. Vietoris, J.L. Elizey, P. Joulain, S.N. Mehta, J.L. Torero, Larminar diffusion flame in microgravity: the results of the Minitexus 6 sounding rocket experiment, Proc. Combust. Inst. 28 (2000) 2883–2889.
[15] A. Paull, H. Alesi, S. Anderson, HyShot flight program and how it was developed, AIAA 2002-4939.
[16] M.K. Smart, N.E. Hass, A. Paull, Flight data analysis of the HyShot 2 scramjet flight experiment, AIAA J. 44 (10) (2006) 2366–2375.
[17] G. Leitmann, A calculus of variation of Goddard's problem, Acta Astronaut. 2 (1956) 55–62.
[18] P. Tsiotras, H. Kelley, Drag-law effects in the Goddard problem, Automatica 27 (3) (1991) 481–490.
[19] H. Seywald, E.M. Cliff, Goddard problem in presence of a dynamic pressure limit, J. Guid. Control Dyn. 16 (4) (1993) 776–781.
[20] K. Graichen, N. Petit, Solving the Goddard problem with thrust and dynamic pressure constraints using saturation functions, in: Proceedings of the 17th World Congress: the International Federation of Automatic Control, Seoul, July 6–11, 2008.
[21] D.D. Ganji, M. Gorji, M. Hatami, A. Hasanpour, N. Khademzadeh, Propulsion and launching analysis of variable-mass rockets by analytical methods, Propuls. Power Res. 2 (3) (2013) 225–233.
[22] S-H. Lee, Analytic approach to determine optimal conditions for maximizing altitude of sounding rocket, Aerosp. Sci. Technol. 40 (2015) 47–55.
[23] S-H. Lee, C.R. Aldredge, Analytic approach to determine optimal conditions for maximizing altitude of sounding rocket: flight in standard atmosphere, Aerosp. Sci. Technol. 46 (2015) 374–385.
[24] US Committee on Extension to the Standard Atmosphere, US standard atmosphere, 1976, NASA-TM-74335.
[25] G.P. Sutton, O. Biblarz, Rocket Propulsion Elements, 7th ed., John Wiley and Sons, 2001.
[26] Howard D. Curtis, Orbital Mechanics for Engineering Student – Chap. 11: Rocket Vehicle Dynamics, 3rd ed., Elsevier Ltd., 2014.
[27] Y. Chen, C. Wen, Z. Gong, M. Sun, Drag coefficient curve identification of projectiles from flight tests via optimal dynamic fitting, Control Eng. Pract. 5 (5) (1997) 627–636.
[28] G.G. Dutta, A. Singhal, A.K. Ghosh, Estimation of drag coefficient from flight data of a cargo shell, in: AIAA Atmospheric Flight Mechanics Conference and Exhibit, AIAA 2006-6149.
[29] S.D. Conte, C. de Boor, Elementary Numerical Analysis: An Algorithmic Approach, 3rd ed., McGraw Hill, 1988.
[30] F.B. Hildebrand, Advanced Calculus for Applications, 2nd ed., Prentice–Hall, 1976, p. 365.